# Zero-width band gap associated with the $\bar{n}=0$ condition in photonic crystals containing left-handed materials

M. de Dios-Leyva and J. C. Drake-Pérez
*Department of Theoretical Physics, University of Havana, San Lázaro y L, Vedado 10400, Havana, Cuba*
(Received 13 November 2008; published 31 March 2009)

We demonstrate that the band structure of a photonic crystal consisting of alternating layers of right-handed material (RHM) and left-handed material (LHM) can exhibit two types of zero-$\bar{n}$ gaps of zero width. It is shown that each type has an associated null-gap condition which determines the scaling properties of the frequency $\nu_0$ at which the corresponding null gap occurs. Specifically, while scaling in the layer thicknesses does not modify the value of the frequency $\nu_0$ determined by one of these conditions, the frequency $\nu_0$ associated with the other one does not exhibit such a scaling behavior. We have also shown that near the touching point $\nu_0$ (for both types of null gaps) and around the center of the Brillouin zone, the dispersion curves exhibit a linear dependence on the Bloch wave vector $k$. As a consequence, the corresponding density of states and group velocity are practically flat as functions of $k$ in the neighborhood of $k=0$. Another interesting property of the considered structure is that an electromagnetic wave with frequency $\nu_0$ can be transmitted through a finite RHM-LHM photonic crystal without any change in amplitude and phase.

DOI: 10.1103/PhysRevE.79.036608 PACS number(s): 41.20.Jb, 42.70.Qs, 78.20.Ci

## I. INTRODUCTION

Left-handed metamaterials (LHMs) represent a novel class of man-made optical materials [1], which have attracted much attention over the past few years. They are very dispersive and have both negative dielectric permittivity $\varepsilon(\omega)$ and negative magnetic permeability $\mu(\omega)$ in some frequency ranges. These artificial composites have a negative index of refraction and are also called double-negative media. The interest in LHMs is motivated by their unusual physical properties [2], such as inverse Snell's law and reversed Doppler and Cherenkov effects, as well as by their vast potential for many applications.

Recent studies indicate that multilayer structures involving LHMs also exhibit unusual physical properties which are mainly determined by the presence of the LHM component in them. In particular, it has been shown [3–10] that one-dimensional (1D) photonic crystals composed of alternating layers of LHM and right-handed material (RHM) may exhibit a new type of band gap possessing a number of unique properties. Such a band gap corresponds to a zero averaged refractive index, $\bar{n}=0$, and its behavior is quite different from that of the conventional photonic crystals. Unlike conventional photonic band gaps originating from the interference of Bragg scattering, the zero-$\bar{n}$ gap is insensitive to the geometrical scaling of the structure and to structural disorder that is symmetric in the random parameters [3]. Further, a more detailed study of the zero-$\bar{n}$ gap revealed that, in general, its properties depend on the physical and geometrical parameters used to characterize the RHM and LHM components of the photonic crystal. In fact, while for a particular choice [5] of these parameters the zero-$\bar{n}$ gap can be an angle-insensitive omnigap for both TE and TM polarizations, a different choice [9,10] does not necessarily lead to a zero-$\bar{n}$ gap possessing such a type of omnigap.

It should be pointed out that the above described properties of the zero-$\bar{n}$ gap were established for photonic crystals with dispersive LHM components, as must be because the LHMs are necessarily dispersive [1]. However, the properties of such a band gap were first studied [11] for the case where both components are nondispersive. In this case, the $\bar{n}=0$ condition is satisfied for all values of $\omega$ and, as shown in Ref. [11] (see also Refs. [3,7]) for normal propagation and impedance mismatch, the corresponding band structure exhibits a band gap (stop band) for all frequencies, except at some discrete values $\omega_m$ which are proportional to the reciprocal of the layer thickness. Due to this, this type of band gap does not exhibit the scaling behavior mentioned in the preceding paragraph. It was also shown that for perfect impedance matching, the structure only exhibits a passband for all frequencies. Thus, it follows from the above discussion that the dispersive properties of the RHM and LHM layers of the photonic crystals play an important role in determining the properties of the zero-$\bar{n}$ gap.

On the other hand, it is clear that the $\bar{n}=0$ condition guarantees the existence of a zero-$\bar{n}$ gap in a RHM-LHM photonic crystal, but it does not determine its width, which depends on the geometrical and physical parameters characterizing the structure. This means that such a photonic crystal can exhibit a zero-$\bar{n}$ gap either of finite or of zero width. The existence of the latter type of band gap was identified in Ref. [10] for oblique propagation and for photonic crystals with dispersive LHM components. The frequency associated with it corresponds to the touching point of two different passbands. Notice, however, that according to the preceding paragraph, the corresponding null gap for photonic crystals with nondispersive components [11] may be identified with the passband mentioned there. Note the difference between the two types of null gaps described above. In the following we focus on photonic crystals with dispersive LHM components and study in detail the properties of the corresponding zero-$\bar{n}$ gap of zero width. In this study we include a detailed analysis of the scaling behavior of it as well as of the zero-$\bar{n}$ gap of finite width. The distribution of electromagnetic modes around the frequency at which the null gap occurs is also studied.

 

The paper is organized as follows. In Sec. II, we derive and discuss the conditions of existence of a zero-$\bar{n}$ gap of zero width. Section III is concerned with the scaling properties of such a null gap. We present in Sec. IV a detailed analysis of the dispersion curves and density of states (DOS) around the frequency $\nu_0$ at which the null gap occurs. A brief discussion of the transmission properties of electromagnetic waves with frequency $\nu_0$ through the considered photonic crystal is presented in Sec. V. Finally, conclusions are given in Sec. VI.

## II. NULL-GAP CONDITIONS

The expressions determining the dispersion relation of a RHM-LHM photonic crystal, for oblique propagation and both TE and TM polarizations of the radiation modes, are well known. It has been shown that they can be written in different equivalent forms. In the study of the properties of the zero-$\bar{n}$ gap, which occurs at the center of the Brillouin zone, it is convenient to use the following form [10]:

$$\sin^2\left(\frac{kd}{2}\right) = q(\omega)r(\omega), \tag{1}$$

where for TE modes the frequency-dependent functions $q(\omega)$ and $r(\omega)$ can be written as

$$q(\omega) = \frac{1}{2}\left\{(1+\tau)\sin\left[\frac{b}{2}\left(\frac{a}{b}Q_1 + Q_2\right)\right] + (1-\tau)\sin\left[\frac{b}{2}\left(\frac{a}{b}Q_1 - Q_2\right)\right]\right\}, \tag{2}$$

$$r(\omega) = \frac{1}{2}\left\{\left(1+\frac{1}{\tau}\right)\sin\left[\frac{b}{2}\left(\frac{a}{b}Q_1 + Q_2\right)\right] + \left(1-\frac{1}{\tau}\right)\sin\left[\frac{b}{2}\left(\frac{a}{b}Q_1 - Q_2\right)\right]\right\}, \tag{3}$$

with

$$Q_1 = \sqrt{\frac{\omega^2}{c^2}\mu_1\varepsilon_1 - q^2}, \quad Q_2 = \sqrt{\frac{\omega^2}{c^2}\mu_2\varepsilon_2 - q^2}, \tag{4}$$

$$\tau = \tau(\omega) = \frac{\mu_2 Q_1}{\mu_1 Q_2}. \tag{5}$$

In these equations, $a$, $\varepsilon_1$, and $\mu_1$ are the width, dielectric permittivity, and magnetic permeability of the RHM layer, respectively. $b$, $\varepsilon_2$, and $\mu_2$ are the corresponding quantities of the LHM layer; $d=a+b$ is the period of the photonic crystal; $k$ is the Bloch wave vector along the axis of the structure, which is limited to the first Brillouin zone $-\pi/d<k<\pi/d$; $n_i=\sqrt{\varepsilon_i}\sqrt{\mu_i}$, with $i=1$ and 2, are the refractive indices; $q$ is the wave-vector component along the lateral direction ($x$ axis); and $Q_1$ and $Q_2$ are the positive components of the wave vector along the stacking direction ($z$ axis). In what follows, we assume that $\varepsilon_1$ and $\mu_1$ are positive and frequency independent. As is well known [9,10], the corresponding expressions for the TM modes are obtained from Eqs. (1)–(5) by interchanging the optical parameters $\varepsilon(\omega)$ and $\mu(\omega)$.

Let us first discuss the conditions for the existence of a zero-$\bar{n}$ gap of zero width. The frequency $\omega_0$ at which the band structure of a RHM-LHM photonic crystal can exhibit such a type of band gap must satisfy the equation [10]

$$\bar{Q}(\omega_0) = \frac{1}{d}[aQ_1(\omega_0) - bQ_2(\omega_0)] = 0. \tag{6}$$

Evaluating the right-hand side of Eq. (1) for $\omega=\omega_0$ and using Eqs. (2)–(6), the Bloch wave vector $k_0$ corresponding to the frequency $\omega_0$ satisfies the equation

$$\sin^2\left(\frac{k_0 d}{2}\right) = \frac{1}{4}\frac{[1+\tau(\omega_0)]^2}{\tau(\omega_0)}\sin^2 aQ_1(\omega_0). \tag{7}$$

If we take into account that for $\omega=\omega_0$, $\mu_2(\omega_0)<0$ and $Q_1(\omega_0)$, $Q_2(\omega_0)$, and $\mu_1$ are positive, the parameter $\tau(\omega_0)<0$ and therefore the right-hand side of Eq. (7) is either negative or equal to zero. In the former case, the wave vector $k_0$ is complex and the structure exhibits a zero-$\bar{n}$ gap (or a zero-$\bar{Q}$ gap) of finite width. In the other case, one of the equations

$$aQ_1(\omega_0) = n\pi, \tag{8}$$

$$\tau(\omega_0) = \frac{\mu_2(\omega_0)Q_1(\omega_0)}{\mu_1 Q_2(\omega_0)} = \frac{\mu_2(\omega_0)}{\mu_1}\frac{b}{a} = -1 \tag{9}$$

is satisfied and a zero-$\bar{Q}$ gap of zero width is formed at the center of the Brillouin zone ($k_0=0$), where $n=1,2,3,\ldots$. Note that the null gap associated with conditions (6) and (9) occurs at a frequency $\omega_0$ which is only dependent on the ratio $a/b$, for a given value of $q$. This means that scaling in the layer thicknesses $a$ and $b$ by an arbitrary factor does not modify the value of $\omega_0$. It should be noted that the frequency $\omega_0$ associated with the conditions (6) and (8) cannot exhibit such a scaling property. In what follows, the null gaps associated with conditions (8) and (9) will be called null gaps of first and second types, respectively.

In the study of the properties of these null gaps, it is important to know the relations between the geometrical and physical parameters of the photonic crystal guaranteeing the occurrence of them. We choose the propagation angle $\theta$ in the RHM layer as one of these parameters, which is related to the wave-vector component $q$ through the relation $q=(n_1\omega/c)\sin\theta$. So, by combining conditions (6) and (8) we obtain the following relations for the null gap of first type:

$$b = \frac{an_1\cos\theta}{\sqrt{\mu_2(\omega_0)\varepsilon_2(\omega_0) - \mu_1\varepsilon_1\sin^2\theta}}, \tag{10}$$

$$\omega_0 = \frac{n\pi c}{an_1\cos\theta}. \tag{11}$$

Similarly, it follows from Eqs. (6) and (9) that the corresponding relations for the null gap of second type are given by

$$\cos^2\theta = \frac{1+(a/b)\varepsilon_2(\omega_0)/\varepsilon_1}{1-(a/b)^2} \quad \text{for } a/b \neq 1, \tag{12}$$

$$\frac{\varepsilon_2(\omega_0)}{\varepsilon_1} = -1 \quad \text{for} \quad a/b = 1, \tag{13}$$

$$\frac{\mu_2(\omega_0)}{\mu_1}\frac{b}{a} = -1. \tag{14}$$

The solutions of Eqs. (10)–(14) play an important role in the study of the formation and properties of the zero-$\bar{Q}$ gap of zero width in RHM-LHM photonic crystals, as we will see later.

It should be pointed out that the results presented above are general enough and can be used to study the properties of the zero-$\bar{Q}$ gap in RHM-LHM photonic crystals for which $\varepsilon_1$ and $\mu_1$ are positive and $\varepsilon_2(\omega)$ and $\mu_2(\omega)$ may follow different configurations. In this paper, we use the effective physical parameters

$$\varepsilon_2(\nu) = 1 + \frac{5^2}{0.9^2 - \nu^2} + \frac{10^2}{11.5^2 - \nu^2}, \tag{15}$$

$$\mu_2(\nu) = 1 + \frac{3^2}{0.902^2 - \nu^2} \tag{16}$$

to model the LHM component of the structure, where $\nu = \omega/2\pi$ is the frequency measured in gigahertz. These optical parameters have been used by various authors [3,9,10] to study the electromagnetic properties of RHM-LHM photonic crystals.

The results obtained from Eqs. (10)–(16) are shown in Fig. 1 for $\mu_1=1$ and two different values of the optical parameter $\varepsilon_1$. Figure 1(a) displays, for $n=1,2$ and $\theta=0$, the dependence of the LHM-layer thickness $b$ on the width $a$ of the RHM layer for the null-gap condition of first type. Note that the domain of definition of $b$ as a function of $a$, for fixed $n$ and $\varepsilon_1$, is a certain region $a>a_0$ of the $a$ axis which depends on $n$ and $\varepsilon_1$. This restriction is determined by the fact that both $\varepsilon_2(\omega)$ and $\mu_2(\omega)$ must be negative at $\omega=\omega_0$. In Fig. 1(b) we display, for $\varepsilon_1=1$ and 4, the dependence of the propagation angle $\theta$ on the ratio $a/b$ for the null-gap condition of second type. Note also that the domain of definition of $\theta$ as a function of the ratio $a/b$ depends on the value of $\varepsilon_1$ considered. In this case, the limitation is determined by the above-mentioned restriction and by the fact that $\theta$ must be a real quantity.

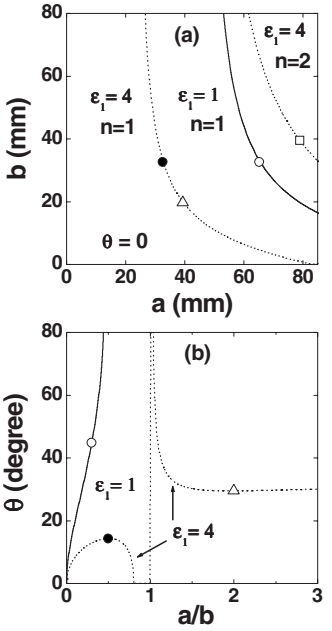


FIG. 1. Results obtained from the null-gap conditions (a) of first type, for $n=1,2$ and $\theta=0$, and (b) of second type, for a photonic crystal composed of alternating layers of a RHM, with optical parameters $\varepsilon_1$ and $\mu_1$, and a LHM with $\varepsilon_2$ and $\mu_2$ given by Eqs. (15) and (16). In both panels, $\mu_1=1$ and solid and dotted lines correspond to $\varepsilon_1=1$ and $\varepsilon_1=4$, respectively. Symbols correspond to particular null-gap points (see text).

## III. SCALING PROPERTIES

Let us now investigate more closely the scaling behavior of the zero-$\bar{Q}$ gap of zero width. In doing so, let us first focus on the scaling properties of the zero-$\bar{Q}$ gap. These properties are not directly determined by the $\bar{Q}(\omega_0)=0$ condition, but by the scaling behavior of its edges. The frequencies associated with these edges are situated around $\omega_0$ and must be solutions of equations $q(\omega)=0$ and $r(\omega)=0$ [see Eq. (1)]. It follows from Eqs. (2) and (3) that for given values of the ratio $a/b$ and $\theta$, such solutions depend in general on the LHM-layer thickness $b$. However, if the conditions

$$aQ_1/2 \ll 1 \quad \text{and} \quad bQ_2/2 \ll 1 \tag{17}$$

are satisfied, the sine functions in Eqs. (2) and (3) can be approximated by their arguments and equations $q(\omega)=0$ and $r(\omega)=0$ reduce (approximately) to

$$\frac{a}{b}Q_1(\omega) + \tau(\omega)Q_2(\omega) = 0, \tag{18}$$

$$\frac{a}{b}Q_1(\omega) + \frac{1}{\tau(\omega)}Q_2(\omega) = 0, \tag{19}$$

respectively. Therefore, the frequencies associated with the mentioned edges are independent of $b$, for fixed values of $a/b$ and $\theta$. Conversely, it follows from equations $q(\omega)=0$ and $r(\omega)=0$ that if the edges of the zero-$\bar{Q}$ gap are independent of $b$, for fixed $a/b$ and $\theta$, conditions (17) are necessarily satisfied. In consequence, the zero-$\bar{Q}$ gap is insensitive to the geometrical scaling of the structure if and only if conditions (17) are satisfied. Of course, when these conditions are violated, the crystal can possess a zero-$\bar{Q}$ gap which does not exhibit such a scaling behavior.

The zero-$\bar{Q}$ gap determined by Eqs. (18) and (19) is of finite width when the solution of Eq. (18) and that of Eq. (19) are different, whereas it is of zero width when these solutions are identical. In the latter case, the bands touch each other at the frequency $\omega=\omega_0$ satisfying Eqs. (6), (18), and (19), implying the zero photonic band-gap condition $\tau(\omega_0)=-1$. Thus, in the limit of small values of the optical

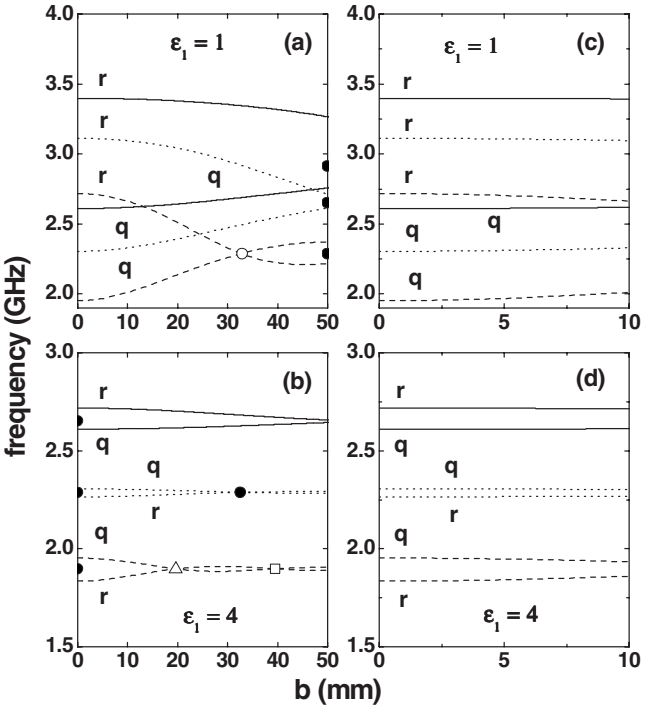


FIG. 2. Frequencies $\nu=\omega/2\pi$ corresponding to the band edges of the zero-$\bar{Q}$ gap as functions of the LHM-layer thickness $b$, for normal propagation, $\varepsilon_1=1,4$, and different values of the ratio $a/b$. In all panels, $\mu_1=1$ and solid, dotted, and dashed lines correspond to $a/b=0.5$, 1, and 2, respectively. Curves $r$ and $q$ represent the edges associated with the zeros of $r$ and $q$, respectively. Solid circles on the vertical axes in panels (a) and (b) correspond to the frequencies $\nu_0=\omega_0/2\pi$ at which $\bar{Q}(\omega_0)=0$. Results in panels (c) and (d) are the same as in (a) and (b), respectively, except that $b\leq 10$ mm. Symbols in panels (a) and (b) correspond to null-gap points (see text).

thickness of the layers, only conditions (6) and (9) are the conditions of existence of a zero-$\bar{Q}$ gap of zero width in a RHM-LHM photonic crystal. This is the expected result because the null gap of first type [see Eqs. (6) and (8)] violates relations (17). It is interesting to note that null-gap conditions (6) and (9) formally coincide with the Alù-Engheta conditions [12,13] which guarantee the existence of a zero-$\phi_{\text{eff}}$ gap of zero width in a single-epsilon-negative and single-mu-negative photonic crystal. The main physical difference between these conditions is associated with the fact that the electromagnetic waves in the Alù-Engheta photonic crystal and in the RHM-LHM photonic crystal are of evanescent and propagating types, respectively.

In order to illustrate the results described above, we first display in Fig. 2 the frequencies $\nu=\omega/2\pi$ associated with the band edges of the zero-$\bar{Q}$ gap, as functions of the LHM-layer thickness $b$, for normal propagation, $\mu_1=1$, and different values of $\varepsilon_1$ and the ratio $a/b$. Curves $r$ and $q$ represent the edges determined by the zeros of $r$ and $q$, respectively. Solid circles on the vertical axes in panels (a) and (b) correspond to the frequencies $\nu_0=\omega_0/2\pi$ at which $\bar{Q}(\omega_0)=0$. In these panels, the geometrical symbol situated at the intersection point of two edges, for a given value of $a/b$, corresponds to a specific null gap of the structure.

As expected, one sees in each one of Figs. 2(a) and 2(b) that for a given value of the ratio $a/b$, the two edges of the zero-$\bar{Q}$ gap are in general varying functions of the LHM-layer thickness $b$, except when the parameter $b$ is small [see Figs. 2(c) and 2(d)]. In the latter case, the zero-$\bar{Q}$ gap is insensitive to the geometrical scaling of the photonic crystal in the considered range of $b$. On the other hand, it is also interesting to note that the band-edge structure depicted in Fig. 2(a), for $\varepsilon_1=1$, is very different from that displayed in Fig. 2(b), for $\varepsilon_1=4$. In fact, when $\varepsilon_1$ goes from 1 to 4, the corresponding zero-$\bar{Q}$ gaps become narrower, and the number of null gaps increases. Moreover, the null gaps shown in Figs. 2(a) and 2(b) are null gaps of first type. This means that corresponding to each of them there is a point in Fig. 1(a). In order to establish clearly which one corresponds to each specific null gap in Fig. 2, for a fixed value of $\varepsilon_1$, we used the same geometrical symbol (open circle, solid circle, etc.) in both figures.

To illustrate the scaling properties of the second-type null gaps, we depict in Fig. 3 the angular dependence of the frequencies corresponding to the band edges of the zero-$\bar{Q}$ gap, for $\mu_1=1$, $\varepsilon_1=1,4$, three different values of the ratio $a/b$, and various values of the LHM-layer thickness $b$. These results were obtained from equations $r(\omega)=0$ and $q(\omega)=0$ [see Eqs. (2) and (3)]. It is clearly seen in each one of Figs. 3(a)–3(c), where the ratio $a/b$ is given, that all edges intersect at a given point $(\nu_0,\theta_0)$ of the $(\nu,\theta)$ plane. Each intersection point corresponds to a null gap of second type because its associated frequency $\nu_0$ is only dependent on the ratio $a/b$. The corresponding null-gap points in Figs. 3 and 1(b) have been identified again with the same geometrical symbol.

One also sees in each one of panels of Fig. 3, where $a/b$ is given, that the width of the zero-$\bar{Q}$ gap is a decreasing function of $b$, for a given value of $\theta\neq\theta_0$. That is, in the ranges of $b$ considered, the zero-$\bar{Q}$ gap is in general sensitive to the geometrical scaling of the structure. This behavior is due to the fact that the corresponding optical thickness of the layers does not satisfy in general conditions (17).

Moreover, one sees from Fig. 3 that, while each $r$ edge is a strongly varying function of $\theta$, the corresponding $q$ edge exhibits in general a slow dependence on $\theta$. It is not difficult to show that the $q$ and $r$ edges determined by Eqs. (18) and (19) exhibit a similar behavior, except that the $q$ edge is always independent of the propagation angle $\theta$. This latter result follows immediately from Eq. (18) if we note that it may be rewritten as

$$\frac{\mu_2(\nu)}{\mu_1}\frac{b}{a}=-1. \tag{20}$$

It is interesting to note that for a given value of the ratio $a/b$, the solution of Eq. (20) coincides with the frequency at which the corresponding null gap in Fig. 3 occurs.

Let us now discuss briefly the properties of the second-type null gap for $a/b=1$. This case was not considered in the preceding discussion because it cannot exist for $\varepsilon_1=1,4$. Substituting Eqs. (15) and (16) into conditions (13) and (14),

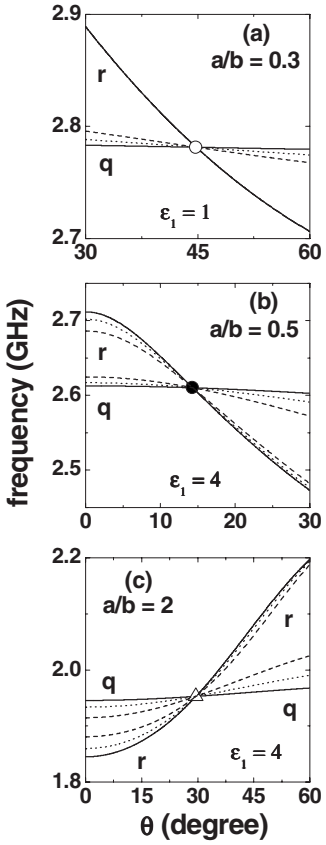


FIG. 3. Angular dependence of the frequencies $\nu=\omega/2\pi$ corresponding to the band edges of the zero-$\bar{Q}$ gap, for $\mu_1=1$ and (a) $a/b=0.3$, with $b=10$ mm (solid lines), $b=20$ mm (dotted lines), $b=30$ mm (dashed lines), and $\varepsilon_1=1$; (b) $a/b=0.5$, with $b=12$ mm (solid lines), $b=20$ mm (dotted lines), $b=30$ mm (dashed lines), and $\varepsilon_1=4$; and (c) $a/b=2$, with $b=6$ mm (solid lines), $b=10$ mm (dotted lines), $b=15$ mm (dashed lines), and $\varepsilon_1=4$. Curves $r$ and $q$ represent the edges determined by the zeros of $r$ and $q$, respectively. Symbols correspond to null-gap points (see text).

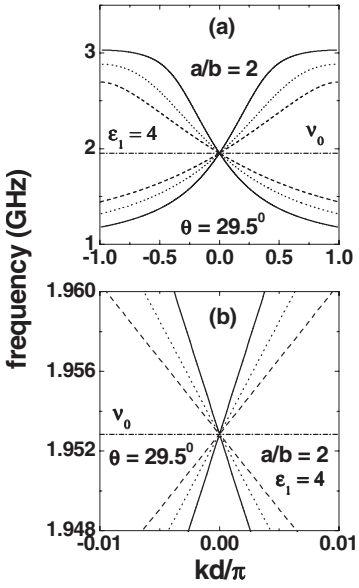


FIG. 4. Dispersion curves around the null gap of second type shown in Fig. 3(c). The frequency $\nu=\omega/2\pi$ is presented as a function of the reduced Bloch wave vector $kd/\pi$, for $a/b=2$, with $b=6$ mm (solid lines), $b=10$ mm (dotted lines), $b=15$ mm (dashed lines), and $\varepsilon_1=4$. Panel (b) displays a magnification of panel (a). The dash-dotted lines represent the frequency $\nu_0$ at which the null gap occurs.

respectively, one can see that for $a/b=1$ and $\mu_1=1$, the corresponding photonic crystal can exhibit such a null gap only when $\varepsilon_1=3.763\,31$. Also, the corresponding bands touch each other at a frequency $\nu_0$, which does not depend on the propagation angle $\theta$; i.e., the touching point $\nu_0$ is independent of $\theta$. A similar situation is met in the study of the Alù-Engheta system [12,13]. Following these authors we refer to conditions (6), (13), and (14), for $a/b=1$, as conjugate matching conditions. This is a case of special significance because, as will be shown below, an electromagnetic wave with frequency $\nu_0$ and any propagation angle $\theta$ can be transmitted through a finite RHM-LHM photonic crystal without any change in amplitude and phase.

## IV. DISPERSION CURVES AND THE DENSITY OF STATES

In order to have a more complete description and better understanding of the considered null gaps, it is important to know how the electromagnetic modes are distributed around the frequency $\omega_0$ at which such a gap occurs. This requires carrying out a detailed study of the properties of the dispersion curves around that frequency. To illustrate these properties, we have calculated from Eq. (1) the two photonic bands associated with the null gap shown in Fig. 3(c). Figure 4(a) displays these bands as a function of the reduced Bloch wave vector $kd/\pi$ for the same parameters $a/b$, $b$, and $\varepsilon_1$ as in Fig. 3(c). Note that the propagation angle $\theta_0$ at which such a null gap occurs is equal to 29.5°. With respect to the results presented in Fig. 4(a), some facts should be pointed out. First, as expected, scaling in the layer thicknesses $a$ and $b$ by an arbitrary factor does not modify the value of $\nu_0=\omega_0/2\pi$. Second, around the center of the Brillouin zone, the frequency $\nu(k)$ is essentially a linear function of the Bloch wave vector $k$, for a given value of $b$. This means that the corresponding group velocity $v_g(k)$, which is determined by the slope of the dispersion curve, is practically independent of $k$ in the neighborhood of $k=0$. Notice also that $v_g(k)$ is a decreasing function of the LHM-layer thickness $b$ (or of $d=a+b$), for a fixed value of $k$ in such a neighborhood. These results are better illustrated in Fig. 4(b), which displays a magnification of the photonic-band structure in Fig. 4(a) in the frequency range containing $\nu_0=\omega_0/2\pi$.

Furthermore, in order to describe appropriately the distribution of electromagnetic modes around the frequency $\omega_0$, it is convenient to derive an analytical expression for the dispersion curves around the center of the Brillouin zone and for $\omega$ near $\omega_0$. The derivation of such an expression is particularly simple if we take into account that $q(\omega_0)=r(\omega_0)=0$. In fact, under these conditions, the frequency-dependent functions $q(\omega)$ and $r(\omega)$ in Eq. (1) can be approximated by $q'(\omega_0)(\omega-\omega_0)$ and $r'(\omega_0)(\omega-\omega_0)$, respectively, and the dis-

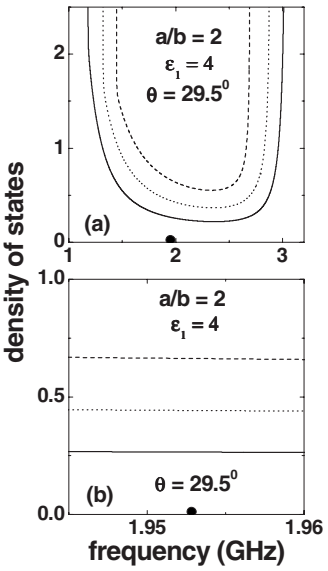


FIG. 5. Density of states associated with the dispersion curves shown in Fig. 4, for $a/b=2$, with $b=6$ mm (solid lines), $b=10$ mm (dotted lines), $b=15$ mm (dashed lines), and $\varepsilon_1=4$. Panel (b) displays a magnification of panel (a). Solid circles on the horizontal axes indicate the frequency $\nu_0$ at which the null gap occurs.

persion curves around the frequencies associated with the null gaps of both types can be written as

$$\omega - \omega_0 = \pm \frac{\pi}{2\sqrt{q'(\omega_0)r'(\omega_0)}} \left| \frac{kd}{\pi} \right|, \tag{21}$$

where the prime denotes differentiation with respect to $\omega$ and the plus and minus signs correspond to the frequency ranges $\omega > \omega_0$ and $\omega < \omega_0$, respectively. It follows from Eq. (21) that $v_g(k) \sim 1/\sqrt{q'(\omega_0)r'(\omega_0)}$.

We turn now to the study of the distribution of electromagnetic modes around the frequencies $\nu_0 = \omega_0/2\pi$ associated with the considered null gaps. Such a distribution is determined by the DOS, which may be defined as the number of Bloch wave vectors $k$ per unit cell of the photonic crystal for a given frequency $\omega$ [14],

$$\rho(\omega) = \frac{1}{N} \sum_k \delta[\omega - \omega(k)], \tag{22}$$

where $N$ is the number of unit cells in the photonic crystal. Replacing the summation over $k$ by an integration and using Eq. (1), the following formula for $\rho(\omega)$ can be obtained:

$$\rho(\omega) = \left| \mathrm{Re}\left( -\frac{1}{2\pi} \frac{df/d\omega}{\sqrt{1-f^2}} \right) \right|, \tag{23}$$

where $f(\omega) = 1 - 2q(\omega)r(\omega)$.

Figure 5(a) displays the DOS obtained from Eq. (23) as a function of the frequency $\nu = \omega/2\pi$ for the same parameters $a/b$, $b$, $\theta$, and $\varepsilon_1$ as in Fig. 4, and in the frequency range where the two bands around the frequency $\nu_0 = \omega_0/2\pi$ are localized. We also show in Fig. 5(b) a magnification of the DOS in Fig. 5(a) in a frequency range containing $\nu_0 = \omega_0/2\pi$.

As one can see from Fig. 5(a), the DOS corresponding to a fixed value of $b$ takes finite values at the touching point $\nu_0$ of the bands, and is infinite at the lower (higher) edge of the first (second) band. These are expected results because $\rho(\omega)$ is proportional to the reciprocal of the group velocity $v_g$ [15], which is finite at $\nu_0$ [see Eq. (21)] and zero at the mentioned edges. From Fig. 5(b) we can also observe that $\rho(\omega)$ is essentially flat as a function of $\nu$ in the considered frequency range. This is also an expected result because, according to Eq. (21), the frequency $\nu(k)$ is essentially a linear function of the Bloch wave vector $k$ in such a range, for a given value of $b$.

## V. TRANSMISSION PROPERTIES

According to the above obtained results, if only condition (6) is satisfied, a zero-$\bar{n}$ gap opens and there is no energy flux in the system when the frequency of the electromagnetic field is inside it. This result also includes the edges of such a gap because the corresponding group velocities are equal to zero. Nevertheless, when the null-gap conditions are satisfied, a zero-$\bar{n}$ gap of zero width is formed at a frequency $\nu_0$ at which the group velocity $v_g$ is different from zero and in general there is an energy flux in the crystal. The latter observation points out the importance of studying the propagation of electromagnetic waves in RHM-LHM photonic crystals when their frequencies are near $\nu_0$. In what follows, we discuss briefly this important point.

As is well known, in the study of the propagation of electromagnetic waves in 1D photonic crystal, it is convenient to use the transfer-matrix method. The usefulness of it is associated with the fact that the transmission of fields through the crystal may be described in terms of the unit-cell transfer matrix $W$, which, for the considered photonic crystal, may be written as

$$W = \begin{bmatrix} W_{11} & \frac{\mu_1}{Q_1} W_{12} \\ -\frac{Q_1}{\mu_1} W_{21} & W_{22} \end{bmatrix}, \tag{24}$$

where

$$W_{11} = \cos aQ_1 \cos bQ_2 - \tau(\omega) \sin aQ_1 \sin bQ_2, \tag{25}$$

$$W_{12} = \sin aQ_1 \cos bQ_2 + \tau(\omega) \cos aQ_1 \sin bQ_2, \tag{26}$$

and $W_{22}$ and $W_{21}$ are obtained from $W_{11}$ and $W_{12}$, respectively, by substituting $\tau(\omega)$ with $1/\tau(\omega)$, where $\tau(\omega)$ is defined in Eq. (5).

It follows immediately from Eqs. (24)–(26) that if one of the null-gap conditions discussed above is satisfied, then $W_{11} = W_{22} = 1$, $W_{12} = W_{21} = 0$, and $W$ in Eq. (24) reduces to the $2 \times 2$ unit matrix. In consequence, an electromagnetic wave with frequency $\nu_0$ (touching point) is transmitted through the unit cell of the photonic crystal without any change in amplitude and phase. This result is remarkable in that it is also valid for the case of a photonic crystal of $N$ unit cells because $W^N$ is the transfer matrix for the system [15]. This means that for $\nu = \nu_0$, the transmission coefficient of the finite

structure (embedded in a host medium) is equal to 1. A similar phenomenon occurs in the Alù-Engheta system (see Refs. [12,13]).

## VI. CONCLUSIONS

In the present work we have demonstrated that the band structure of a RHM-LHM photonic crystal can exhibit two types of zero-$\bar{n}$ gaps of zero width. Each type has an associated null-gap condition which determines the properties of the corresponding null gap, including the scaling properties of the frequency $\nu_0$ at which it occurs. In fact, while scaling in the layer thicknesses does not modify the value of the frequency $\nu_0$ determined by one of these conditions, the frequency $\nu_0$ associated with the other one does not exhibit such a scaling behavior. On the other hand, we have also shown that near the touching point $\nu_0$ (for both types of null gaps) and around the center of the Brillouin zone, the dispersion curves exhibit approximately a linear dependence on the Bloch wave vector $k$. As a consequence, the corresponding density of states and group velocity are practically flat as functions of $k$ in the neighborhood of $k=0$. Another interesting property of the considered structure is that an electromagnetic wave with frequency $\nu_0$ can be transmitted through a finite RHM-LHM photonic crystal without any change in amplitude and phase.

Finally, we believe that the obtained results and associated discussion can be of special significance for band-gap engineering and related applications. In particular, the obtained null-gap conditions as well as the established properties of the DOS and group velocity may be useful for the design of RHM-LHM photonic crystal devices.

## ACKNOWLEDGMENTS

This work was partially supported by an Alma Mater Project of the University of Havana. We would like to thank R. L. Soto Morán for critically reading the paper.

[1] S. A. Ramakrishna, Rep. Prog. Phys. **68**, 449 (2005).
[2] V. G. Veselago, Sov. Phys. Usp. **10**, 509 (1968).
[3] J. Li, L. Zhou, C. T. Chan, and P. Sheng, Phys. Rev. Lett. **90**, 083901 (2003).
[4] L. Wu, S. He, and L. Shen, Phys. Rev. B **67**, 235103 (2003).
[5] H. Jiang, H. Chen, H. Li, and Y. Zhang, Appl. Phys. Lett. **83**, 5386 (2003).
[6] I. V. Shadrivov, A. A. Sukhorukov, and Y. S. Kivshar, Appl. Phys. Lett. **82**, 3820 (2003).
[7] D. Bria, B. Djafari-Rouhani, A. Akjouj, L. Dobrzynski, J. P. Vigneron, E. H. El Boudouti, and A. Nougaoui, Phys. Rev. E **69**, 066613 (2004).
[8] N. C. Panoiu, R. M. Osgood, Jr., S. Zhang, and S. R. J. Brueck, J. Opt. Soc. Am. B **23**, 506 (2006).
[9] H. Daninthe, S. Foteinopoulou, and C. M. Soukoulis, Photonics Nanostruct. Fundam. Appl. **4**, 123 (2006).
[10] M. de Dios-Leyva and O. E. González-Vasquez, Phys. Rev. B **77**, 125102 (2008).
[11] I. S. Nefedov and S. A. Tretyakov, Phys. Rev. E **66**, 036611 (2002).
[12] A. Alù and N. Engheta, IEEE Trans. Adv. Packag. **51**, 2558 (2003).
[13] S. Zouhdi, A. V. Dorofeenko, A. M. Merzlikin, and A. P. Vinogradov, Phys. Rev. B **75**, 035125 (2007).
[14] K. Busch, M. Frank, A. Garcia-Martin, D. Hermann, S. F. Mingaleev, M. Schillinger, and L. Tkeshelashvili, Phys. Status Solidi A **197**, 637 (2003).
[15] J. M. Bendickson, J. P. Dowling, and M. Scalora, Phys. Rev. E **53**, 4107 (1996).